ELSEVIER

Journal of Luminescence 82 (1999) 241–249

JOURNAL OF LUMINESCENCE

Luminescence properties of Sm^{2+} in barium octaborates ($BaB_8O_{13}:Sm^{2+}$)

Qinghua Zeng[a,*], Zhiwu Pei[a], Qiang Su[a], Shaozhe Lu[b]

[a]*Laboratory of Rare Earth Chemistry and Physics, Changchun Institute of Applied Chemistry, Chinese Academy of Sciences, Changchun, Jilin 130022, People's Republic of China*

[b]*Laboratory of Excited State Processes, Changchun Institute of Physics, Chinese Academy of Sciences, Changchun 130021, People's Republic of China*

Received 13 November 1998; received in revised form 24 March 1999; accepted 29 March 1999

Abstract

The luminescence of Sm^{2+} in BaB_8O_{13} are studied as a function of temperature. At 10 K, several crystallographic sites for Sm^{2+} ions with inversion symmetry are possible and $^5D_0 \rightarrow {}^7F_1$ transition show predominant intensities, whereas above 50 K two crystallographic sites without inversion symmetry are clearly observed for Sm^{2+} in BaB_8O_{13} and the $^5D_0 \rightarrow {}^7F_0$ transition show strongest intensity. The vibronic transitions and the non-radiative transitions of Sm^{2+} are studied and a coupled-phonon energy about $50\,cm^{-1}$ is obtained. The thermal effects on the line shift, emission intensities, half-width and lifetime of the $^5D_0 \rightarrow {}^7F_0$ transition are also studied. The decay curves at different temperatures are all in single exponential and are temperature-independent with lifetime around 3.5 ms.

Keywords: Sm^{2+}; Barium borates

1. Introduction

It was reported that Eu^{3+}, Sm^{3+}, Yb^{3+} and Tm^{2+} could be reduced to the corresponding divalent lanthanide ions in SrB_4O_7 by solid state reaction at high temperature in air [1,2]. It is proposed that the rigid three-dimensional network of BO_4 tetrahedra is a unique structure to stabilize the divalent rare-earth ions at high temperature in an oxidizing atmosphere. The BaB_8O_{13} structure is built up by two separate interlocking three-dimensional infinite networks as triborate and pentaborate groups and forms BO_3 and BO_4 tetrahedral units [3]. It is also expected that the BaB_8O_{13} is a suitable host for the luminescence of divalent lanthanide ions.

In this paper the luminescence of Sm^{2+} in BaB_8O_{13} and the temperature effects on the $^5D_0 \rightarrow {}^7F_0$ transition of Sm^{2+} in the host are reported. The vibronic transitions of Sm^{2+} are also studied.

2. Experimental

The samples of BaB_8O_{13} doped with lanthanide ions were prepared by a mixture of analytical-grade

* Corresponding author. Tel.: 0086-431-5682801; fax: 0086-431-5685653.

E-mail address: zengqh@ns.ciac.jl.cn (Q. Zeng)

0022-2313/99/$ - see front matter
PII: S0022-2313(99)00041-1

barium carbonates and boric acid (3 mol% excess). The concentration of the dopant Sm_2O_3 (99.99%) is 2 mol%. The mixtures were heated in air at 400°C for 3 h and 800°C for 15 h.

The crystal structure was checked by X-ray powder diffraction using Cu $K_{\alpha 1}$ radiation. Samples appeared to be single phase. The low-resolution spectra were recorded on a SPEX DM3000F spectrofluorometer equipped with 0.22 m SPEX 1680 double monochromators (resolution 0.1 nm) and a 450 W xenon lamp as excitation source. The excitation power output was corrected. The high-resolution spectra and decay time are recorded with Spex-1403 spectrophotometer under the excitation of N_2 laser beam (337.1 nm) (National Research Instruments Co.) with cryostat of gaseous helium. The temperature could be varied from 10 to 300 K. The high-temperature luminescence are recorded by a Hitachi MPF-4 spectrofluorometer with 150 W xenon lamp as excitation source and a self-assembled furnace as heating source. The temperature can be varied in the range 300–573 K.

3. Results and discussion

3.1. The luminescence of Sm^{2+} in BaB_8O_{13}

The sample $BaB_8O_{13}:Sm^{2+}$ exhibits efficiently deep red emission under UV excitation. The emission spectra of $BaB_8O_{13}:Sm^{2+}$ are recorded at different temperatures under 337.1 nm excitation. It is found that the spectra change appreciably with temperatures. Fig. 1 shows the spectra at 10 and 50 K. Firstly, our attention turns to the luminescence at 50 K. Due to the effect of the crystal field, the energy levels of divalent samarium are split into several sublevels and all the transitions therefore consist of a multiplicity of lines corresponding to the transitions between different sublevels. As shown in Fig. 1b, there are three group lines in the range 14640–14740, 14430–14190 and 14000–13690 cm^{-1} which, respectively, correspond to the transitions between the $^5D_0$ level and ^7F_J ($J = 0,1,2$) multiplets of Sm^{2+}. In the $^5D_0 \rightarrow {}^7F_0$ transition, two lines at 14642 (center I) and 14740 cm^{-1} (center II) appear with the strongest intensities among all the transitions. This

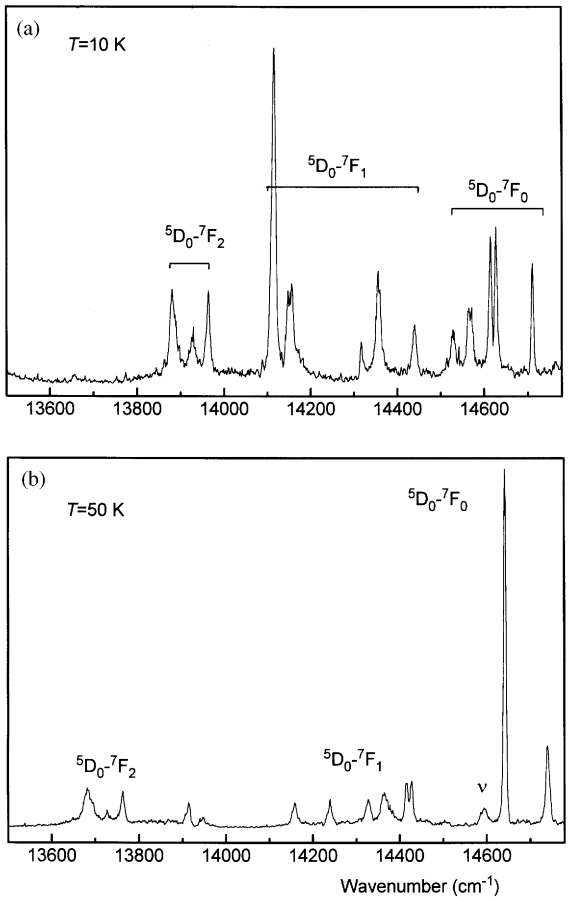

Fig. 1. The emission spectra of Sm^{2+} in BaB_8O_{13} at (a) 10 K and (b) 50 K.

reveals that Sm^{2+} ions occupy the crystallographic sites without inversion symmetry. In the $^5D_0 \rightarrow {}^7F_1$ transition, the degeneracy of $^7F_1$ energy level for both sites is completely lifted and six well-separated lines at 14428, 14417, 14365, 14328, 14240, 14189 cm^{-1} are observed. The $^5D_0 \rightarrow {}^7F_2$ transition is not resolved well with sufficient accuracy. Two lines in $^5D_0 \rightarrow {}^7F_0$ transition reveals the fact that two different crystallographic sites are possible for Sm^{2+} in the host lattice, even though it was reported that there is only one site in the host [3]. This result on the number of the crystallographic sites in the host is in agreement with those reported in literature [4] which was confirmed later by the luminescence of co-doped $BaB_8O_{13}:Ce^{3+}$,

Mn^{2+} [5]. The authors [5] reported that the Mn^{2+} ions showed two emission bands at 520 nm (green emission) and 600 (red emission) under the UV excitation. Thereby, Mn^{2+} ions occupy two crystallographic sites: one on octahedral Ba^{2+} site with coordination number CN = 6 (red emission) and the other on the tetrahedral boron position (BO_4 units) with CN = 4 (green emission). Due to the large different ionic radii between Sm^{2+} and B^{3+} ions, one can expect that the amount of the substitution of Sm^{2+} on B^{3+} position will be much less than on Ba^{2+} sites and its emission intensity will be weaker. This is really the case as shown in the emission spectrum and then we can deduce that center I corresponds to the octahedral Sm^{2+} in Ba^{2+} and center II to tetrahedral B^{3+} position. The occupancy of Sm^{2+} on B^{3+} will cause a serious distortion and the extra charge for Sm^{2+} in B^{3+} position is compensated by defect.

The luminescence of Sm^{2+} in the host at 10 K shown in Fig. 1a is drastically different from those at 50 K. The spectrum consists of large number of sharp lines. Their difference lie not only in the line positions but also in the transition intensities. Due to the limitation of the experimental setups, some lines are not resolved well. However, on the basis of their energetic positions, the spectra may be divided into three groups: Group 1 consists of lines from $\sim 14\,780$ to $14\,500\ cm^{-1}$ corresponding to the $^5D_0 \rightarrow {}^7F_0$ transition. Group 2 has lines from $\sim 14\,500$ to $14\,000\ cm^{-1}$ corresponding to the $^5D_0 \rightarrow {}^7F_1$ transition, while the lines from $\sim 14\,000$ to $13\,600\ cm^{-1}$ belong to Group 3 corresponding to the $^5D_0 \rightarrow {}^7F_2$ transition. In Group 1, more than five distinct lines can be observed. These lines should originate from different crystallographic sites. This means that due to the low temperature the sublattice of Sm^{2+} in the host is thereby distinguishable. This may be reasonable since the ionic radius for Sm^{2+} is smaller than that for Ba^{2+} and the substitutions of Ba^{2+} site by Sm^{2+} will lead to slightly local distortions in lattice. Thus, one can expect that the ligands around the Sm^{2+} ion in the host are distorted from the equilibrium host crystal positions. The random distribution of these distorted positions will therefore give rise to the $^5D_0 \rightarrow {}^7F_0$ transition lines at different energy at such low temperature. The line at $14\,116\ cm^{-1}$ in Group 2 has the strongest intensity at this temperature. This is contrast to the spectra at 50 K in which the line at $14\,642\ cm^{-1}$ is the strongest one. The dominant luminescent centers at this temperature are therefore mostly in sites with inversion symmetry. With increasing temperature, the emission lines in some centers become undistinguishable and overlapped while those in some other centers are probably quenched by temperature.

The low-resolution excitation and emission spectra of Sm^{2+} in BaB_8O_{13} at room temperature are shown in Fig. 2. The excitation spectrum peaking at about 355 nm corresponds to the $4f^5d \rightarrow 4f^6$ transition in Sm^{2+}. The excitation of divalent

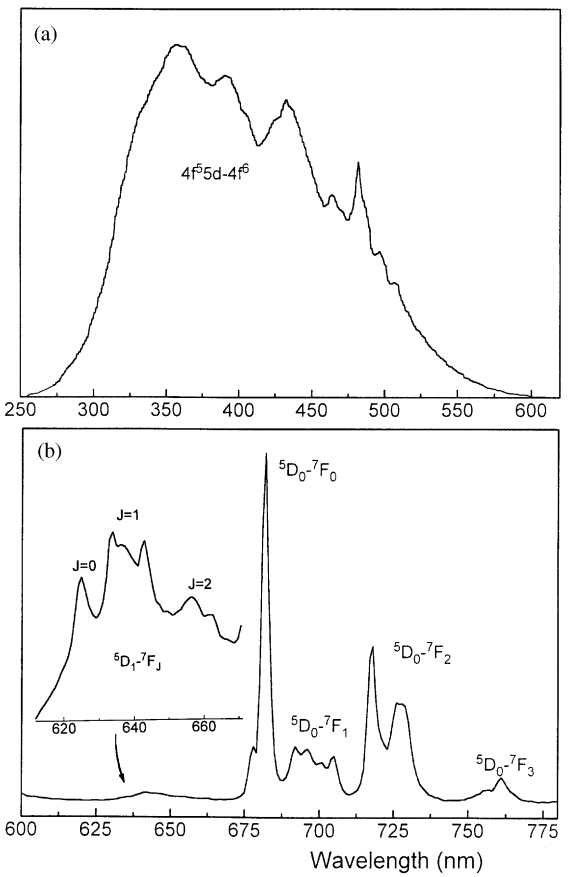

Fig. 2. The low-resolution (a) excitation ($\lambda_{em} = 682$ nm) and (b) emission spectra ($\lambda_{ex} = 355$ nm) of Sm^{2+} in BaB_8O_{13} at room temperature (the inset shows enlargement of the emission spectrum in the range 620–670 nm).

samarium takes place via the strong $4f^5 5d$ bands from which the ions quickly decay to the lower metastable level. From the position of the excitation band, it is suggested that the $4f^5 5d$ levels of Sm^{2+} in BaB_8O_{13} be located in relatively higher energy position than in alkaline earth halides [6–8]. This is due to the fact that in BaB_8O_{13} the boron atoms are coordinated with oxygen in sp^3 hybrid orbital and form BO_4 three-dimensional units [3]. Such structure is thought to be a rigid one which can oppose relaxation in the excited state of the divalent rare-earth ions since the stiffness of the host will prevent the energy from being transferred to the host vibrations [9,10]. The sharp lines appeared in the excitation band correspond to the ^6H_J ($J = \frac{13}{2}, \frac{11}{2}, \frac{9}{2}, \frac{7}{2}$) states of the $4f^5$ configuration since the splitting of $4f^5$ configuration was well known in the spectroscopy of the Sm^{3+} free ion [11] and therefore, similarities in the spectra of Sm^{2+} are expected. In the emission spectrum, besides the f–f transitions in the range 680–780 nm corresponded to $^5D_0 \rightarrow {}^7F_J$ ($J = 0, 1, 2, 3$) multiplets, some other lines appear in the range 620–670 nm (shown in the inset in Fig. 2) which ascribe to the $^5D_1 \rightarrow {}^7F_J$ ($J = 0, 1, 2, 3$) of Sm^{2+} in the host (discussed below).

3.2. The vibronic transitions of Sm^{2+}

An excited impurity ion in a lattice can lose its energy by spontaneous photon, phonon-assisted emission, or by non-radiative transitions. They are temperature-dependent and arise from vibrational-electronic or 'vibronic' interactions. The relative contributions of the vibronic and purely radiative transitions to the de-excitation can be found directly by measuring the intensities of the vibronic and non-phonon emission lines as a function of temperature [12]. In Fig. 3 are shown the enlargements of the high-resolution spectra of Sm^{2+} in BaB_8O_{13} at different temperatures. A weak line (denoted v in Spectrum a) at 14 592 cm^{-1}, which is about 50 cm^{-1} lower in energy than the $^5D_0 \rightarrow {}^7F_0$ (14 642 cm^{-1}) transition can be observed. At 150 K another weak line (denoted v') on the higher energy side of the $^5D_0 \rightarrow {}^7F_0$ transition with almost the same 50 cm^{-1} energy displacement appears. These two lines increase in intensity and broaden with increasing temperature and overlapped with the $^5D_0 \rightarrow {}^7F_0$ transition at 300 K. The position of the $^5D_0 \rightarrow {}^7F_0$ transition shifts to higher energy side with increasing temperature; hence, the positions of these two weak lines v and v' also shift in the same direction, but the difference in energy between each line and the $^5D_0 \rightarrow {}^7F_0$ line does not change. Because there are only two sites for divalent samarium in BaB_8O_{13}, these weak lines cannot be the transitions of Sm^{2+} in different sites, line v and v' should be assigned to phonon satellite lines which coupled with the zero-phonon line (ZPL) ($^5D_0 \rightarrow {}^7F_0$) during the transition between these two energy levels: $|{}^5D_0, n\rangle \rightarrow |{}^7F_0, n+1\rangle$ and $|{}^5D_0, n+1\rangle \rightarrow$

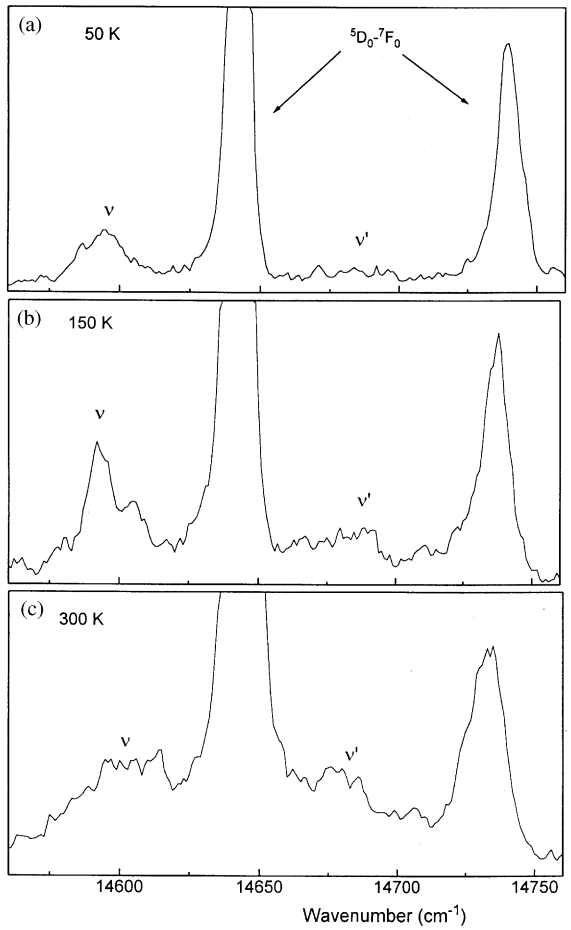

Fig. 3. The phonon satellite lines of Sm^{2+} in BaB_8O_{13} at (a) 50 K, (b) 150 K and (c) 300 K.

$|^7F_0, n\rangle$, respectively, where n is the quantum number of the vibrational levels of the crystal lattice. This vibration is a vibrational mode in which Sm moves relative to the borate group [9]. The intensity of v and v' also increase with increasing temperature as shown in Fig. 3. The Huang–Rhys factor S (electron–phonon coupling strength) which can be calculated from the relative intensities of the phonon satellite and ZPL is about 0.03 [13–15].

Vibronic transitions of rare-earth ions arise from the coupling of the $4f^n$ state with the infrared-active vibrational modes (electron–phonon coupling) of the lattice in which the parity selection rule of the purely electronic f–f transitions is broken. The electron–phonon coupling strength usually depends on the covalency, the polarizability and the admixture of the states having the opposite parity [12]. These factors are responsible for the variation in the vibronic transition probability and the multiphonon relaxation rate. In $4f^n$ ions, such coupling with 4f electrons is often weak due to the well shielding by the outer $5s^25p^6$ electrons, but it has a large influence on the optical properties of rare-earth ions. The shape of the vibronic spectra is mainly governed by the electron–phonon interactions. When this interaction is weak, the spectra will be dominated by sharp lines; when this interaction is strong, then structureless bands are observed [11]. In the f–f transitions of $4f^n$ ions, this interaction is usually weak and sharp vibronic transition lines will appear. However, this is not always the case. The interaction will also change in different lattice. In the spectra of Sm^{2+} in $BaCl_2$ and $BaBr_2$, a wide vibronic sideband which stretches from ZPL to $\sim 200\,cm^{-1}$ is found [6]. These vibronic sidebands are caused by the lattice vibrations in the anion sublattices. All of the vibrational modes in the lattice are coupled with the transitions and result in a wide continuous band. In $BaB_8O_{13}:Sm^{2+}$, we do not find such continuous band but only sharp phonon lines are found beside ZPL. During the transition process, only the vibration mode with single frequency is coupled with the 4f electrons and results in sharp and weak lines.

At all temperatures below 300 K, no $^5D_1 \rightarrow {}^7F_J$ transitions are found, even so at 10 K. This is contrast to the spectra of Sm^{2+} in $BaCl_2$, $BaBr_2$ [6]. In these alkaline earth halides, Sm^{2+} shows the $^5D_1 \rightarrow {}^7F_J$ transitions at low temperature and are gradually quenched with increasing temperature. These differences are owing to the different vibrational energy in the host lattice, which lead to different radiative and non-radiative transition rates from $^5D_1$ to $^5D_0$ level. The non-radiative transition rate (A_{NR}) from $^5D_1$ to $^5D_0$ can be roughly estimated by [14,15]:

$$A_{NR} = N\frac{[1-\exp(-\hbar\omega/kT)]^{-p}S^p}{P!} \times \exp\left[\frac{-2S}{1-\exp(-\hbar\omega/kT)}\right].$$

Here S is Huang–Rhys factor; k is the Boltzmann constant; $\hbar\omega$ is the phonon energy involved; T is the absolute temperature; P is the number of the phonons involved ($P<0$ stands for absorption of P phonons and $P>0$ for emission of P phonons); N is the rate constant of the non-radiative transition within the order of $10^{14}\,s^{-1}$, and $P_0 = (\Delta E_{1-0}/\hbar\omega)$ (P_0 is the number of the phonons bridging the energy difference ΔE_{1-0} between the $^5D_1$ and $^5D_0$ level); Because the positions of the $^5D_1$ and $^5D_0$ levels in Sm^{2+}-doped matrix do not change greatly, the energy difference between the $^5D_1$ and $^5D_0$ level is about $\Delta E_{1-0} \approx 1350\,cm^{-1}$. Different lattices have different phonon energies $\hbar\omega$, so P_0 will be different in different lattices. Therefore, the non-radiative transition rate will change with different lattices. During the non-radiation de-excitation process, the phonon with the highest frequency will play the dominant role, and the non-radiative transition rate will mostly be determined by this phonon [16]. The maximum phonon energy in BaB_8O_{13} is about $\hbar\omega \approx 1200 \sim 1400\,cm^{-1}$ of asymmetric and symmetric stretching mode of the BO_3 and BO_4 units [3,17], therefore the number of the phonons is $P_0 \approx 1$, and then the highest possible non-radiative transition rate A_{NR} can be calculated about $7.50\times10^{13}\,s^{-1}$. In weak coupling, the non-radiative transition rate increases sharply with the maximum phonon energy $\hbar\omega$. For example, in $BaCl_2:Sm^{2+}$ [6], the maximum phonon energy is $\hbar\omega \approx 210\,cm^{-1}$, and the number of the phonons is $P_0 \approx 6 \sim 7$. Therefore, the non-radiative transition rate from $^5D_1$ to $^5D_0$ level in BaB_8O_{13} is about

10^{15} times higher than in $BaCl_2$. This comparison reveals the fact why no optical transitions from $^5D_1$ to ^7F_J levels are observed even at 10 K for Sm^{2+} in BaB_8O_{13}, while those transitions can still be observed even at 77 K for Sm^{2+} in $BaCl_2$.

However, contradicted with the above observation and the calculation of the non-radiative transition rate (A_{NR}), an interesting phenomenon is found that a group lines appear in the range 620–670 nm at room temperature (see the inset in Fig. 1). This spectrum is in the form of sharp, though weak lines. On the consideration of their positions, these lines must correspond to the $^5D_1 \rightarrow {}^7F_J$ (0, 1, 2) transitions of Sm^{2+} in the host. At first glance, it conflicts with the usual result that, generally, the $^5D_1 \rightarrow {}^7F_J$ ($J = 0, 1, 2$) transitions are previously quenched by temperature before the $^5D_0 \rightarrow {}^7F_J$ ($J = 0, 1, 2$) transitions (two-step fluorescence quenching mechanism [6]), while in the present case, the $^5D_1 \rightarrow {}^7F_J$ transitions appeared at room temperature. The vibrational mode of BO_4 and BO_3 is at around 1200–1400 cm^{-1} [17] which is very close to the energy gap between $^5D_1$ and $^5D_0$ level ($\Delta E \approx 1350\ cm^{-1}$). This energy gap can be bridged by only one phonon and therefore, the non-radiative transition probability from $^5D_1$ to $^5D_0$ level must be very high and no transitions between $^5D_1$ and ^7F_J could be observed as discussed above. This appearance is explained that the $^5D_1$ level is thermally populated by the $^5D_0$ level via $4f^5 5d$ level, and therefore, the transition sequence becomes $^5D_0 \rightarrow {}^5D_1 \rightarrow {}^7F_J$. The indirect $^5D_1 \rightarrow {}^5D_0$ non-radiative channel through 5d band was considered to be a novel situation and a direct $^5D_1 \rightarrow {}^5D_0$ coupling should be more likely event due to the relatively close proximity of these two J levels [6]. This explanation is confirmed by the high-temperature luminescence of the $^5D_0 \rightarrow {}^7F_J$ and $^5D_1 \rightarrow {}^7F_J$. Fig. 4 shows the temperature effects on the integrated emission intensities of the $^5D_0 \rightarrow {}^7F_J$ and $^5D_1 \rightarrow {}^7F_J$ ($J = 0, 1, 2$) transitions in the range 300–573 K. It can be observed that the intensities of $^5D_1 \rightarrow {}^7F_J$ increase with temperature and those of $^5D_0 \rightarrow {}^7F_J$ decrease. When the temperature is around 370 K, the intensities of $^5D_0 \rightarrow {}^7F_J$ starts to decrease due to the thermal quenching. At around 450 K, the $^5D_{0,1} \rightarrow {}^7F_J$ transitions are almost completely quenched by temperature.

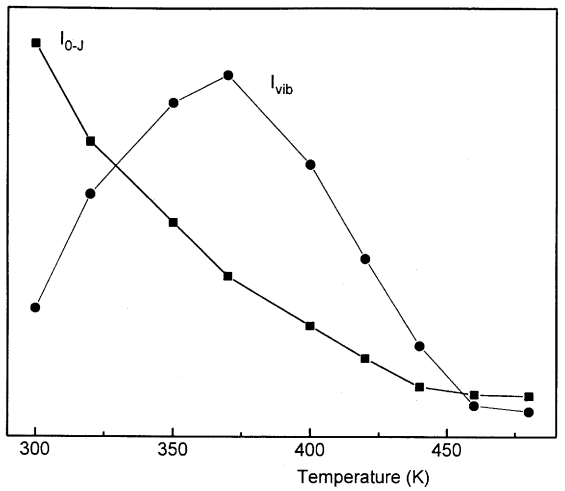

Fig. 4. The temperature effects on the integrated emission intensities of the $^5D_0 \rightarrow {}^7F_J$ and $^5D_1 \rightarrow {}^7F_J$ ($J = 0, 1, 2$) transitions of Sm^{2+} in BaB_8O_{13} between 300 and 473 K.

3.3. The temperature dependence of the $^5D_0 \rightarrow {}^7F_0$ transition

Thermal effects on the $^5D_0 \rightarrow {}^7F_0$ transition of Sm^{2+} in BaB_8O_{13} are studied at different temperatures between 50 and 300 K. The temperature dependence of the line shift and half-width of the $^5D_0 \rightarrow {}^7F_0$ transition are illustrated in Fig. 5. It can be found that the position of center I undergo red shifts as temperature increases whereas that of center II shows green shifts. The half-width also increase with increasing temperature due to the thermal broadening. The thermal effects on line shift should be due to the metastable state of $4f^5 5d$ configuration within Sm^{2+} since the electronic charge is strongly affected by the thermal perturbations of the environment. The thermal broadening is due to static and random microscopic strains and Raman scattering of phonons [18]. The thermal effects on the integrated emission intensities of the $^5D_0 \rightarrow {}^7F_0$ transition are also studied between 50 and 300 K and shown in Fig. 6. The results show that the emission intensities of center I increase with increasing temperature. However, the intensities of center II is not found to change in a fixed way in our results.

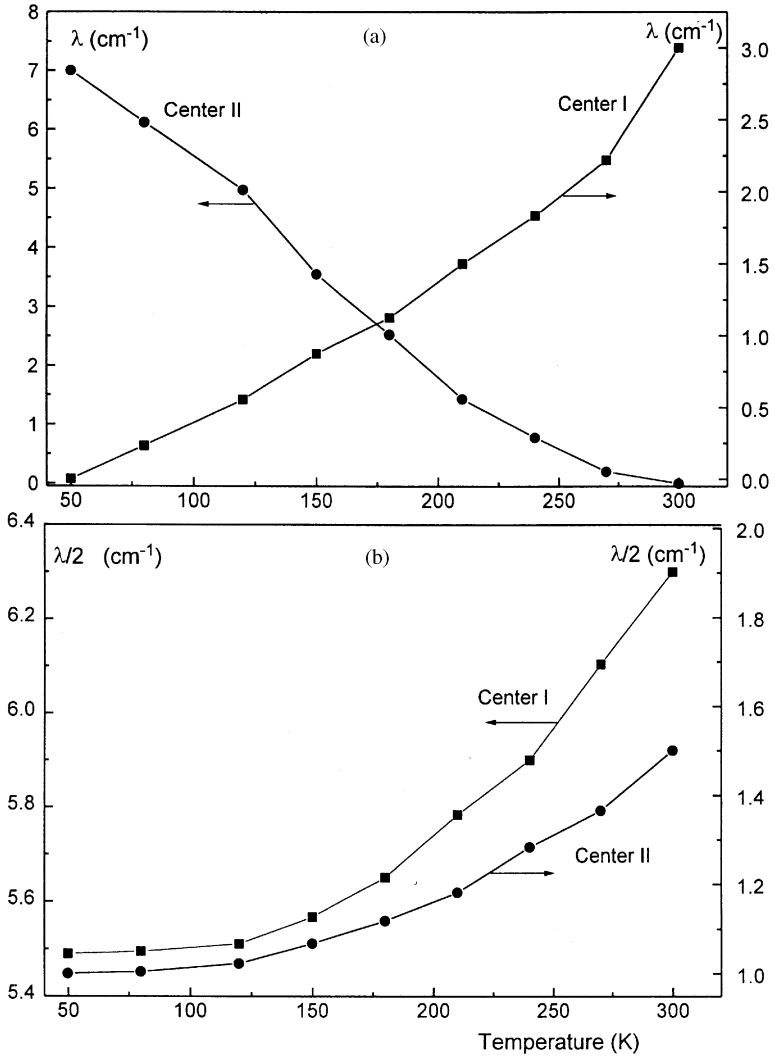

Fig. 5. The temperature dependence of (a) the positions and (b) half-width of the $^5D_0 \rightarrow {}^7F_0$ transition of Sm^{2+} in center I and center II in BaB_8O_{13}.

The lifetime measurements can yield information about the kinetic of the luminescence process, such as the fluorescence efficiency, energy transfer, the excitation and de-excitation process. The decay curves of $^5D_0 \rightarrow {}^7F_0$ transition in center I are recorded as a function of temperature. The results show that the lifetime is temperature-independent: at 200 K, $\tau \approx 3.7$ and at 300 K, $\tau \approx 3.4$ ms. Fig. 7 shows the decay curve at 50 K. The decay curve is single exponential with lifetime of 3.5 ms. This result seems to be contradictory with the temperature dependence of the emission intensities as shown above that the intensities increase with temperature. Theoretically, the lifetime should be prolonged with the increase in population number in the $^5D_0$ levels. Such a contradiction may be explained by the fact that the radiative decay rate increases with the increase in temperature and that the decrease in decay time is compensated by this increase. Therefore, the decay behavior is temperature independent.

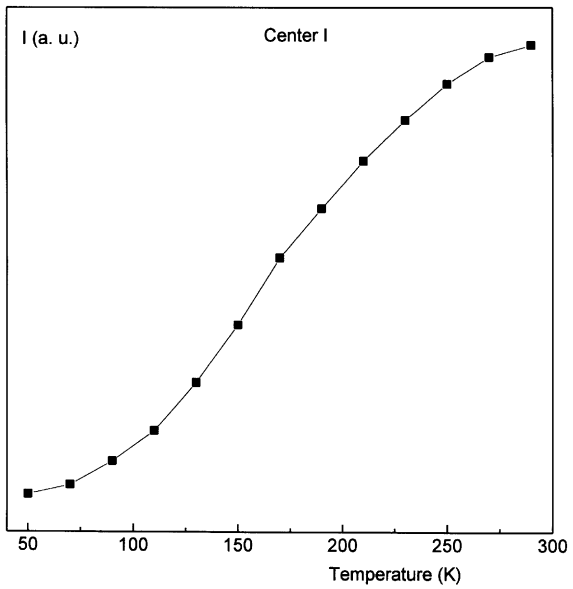

Fig. 6. The thermal effects on the emission intensities of the $^5D_0 \rightarrow {}^7F_0$ transition of Sm^{2+} in center I in BaB_8O_{13}.

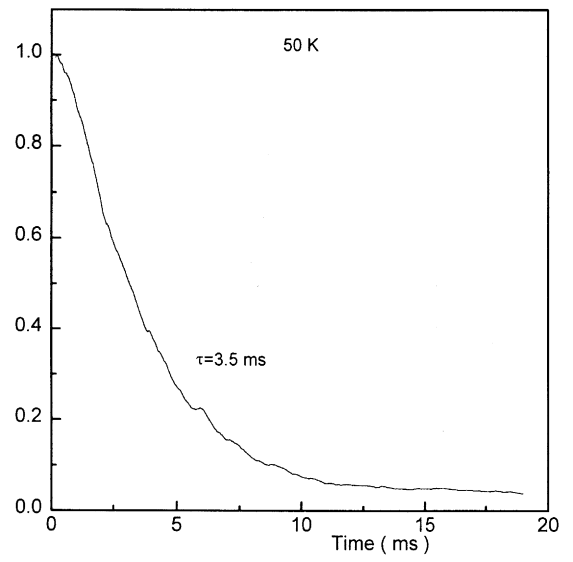

Fig. 7. The decay curve of the $^5D_0 \rightarrow {}^7F_0$ transition of Sm^{2+} in center I in BaB_8O_{13} at 50 K.

4. Conclusions

The investigation on valence change and luminescence of samarium ions in BaB_8O_{13} shows that the matrix BaB_8O_{13} is a good host for the luminescence of the divalent samarium ions. At 10 K, at least five crystallographic sites with inversion symmetry for Sm^{2+} are available and the $^5D_0 \rightarrow {}^7F_1$ transition shows the predominant intensities. At 50 K, two crystallographic sites without inversion symmetry for Sm^{2+} are possible at 50 K in BaB_8O_{13}: one on octahedral coordinated Ba^{2+} site and the other on tetrahedral coordinated B^{3+} position. The phonon–electron coupling energy is about 50 cm^{-1} and an approximate calculation on the non-radiative transition rate of Sm^{2+} explains why no $^5D_1 \rightarrow {}^7F_J$ transitions can be observed even at low temperature. However, due to the thermal population, the $^5D_1 \rightarrow {}^7F_J$ transitions appear again at room temperature even though the vibration of borate is in high energetic frequency which is very close to the energy gap between the $^5D_1$ and $^5D_0$ levels. From the observed temperature dependence on the $^5D_0 \rightarrow {}^7F_0$ transition, it is shown that with increasing temperature the $^5D_0 \rightarrow {}^7F_0$ transition of center I at 14 642 cm^{-1} shifts to higher energy side whereas center II at 14 740 cm^{-1} shifts toward lower energy side. The decay curves are all in single exponential in the temperature range investigated and the lifetime is temperature-independent with values about 3.5 ms. The study on the luminescence of Sm^{2+} in this host has shown that the vibrational phonon plays a significant role in the non-radiative transitions and in the $^5D_1$–$^7F_0$ transitions at higher temperature.

Acknowledgements

This work is supported by the National Natural Foundation of China and the Laboratory of Excited State Processes of the Chinese Academy of Sciences.

References

[1] Z. Pei, Q. Su, J. Zhang, J. Alloys Compounds 198 (1993) 51.
[2] J.R. Peterson, W. Xu, S. Dai, Chem. Mater. 7 (1995) 1686.
[3] J. Krogh-Moe, M. Ihara, Acta Crystallogr. B 25 (1969) 2153.

[4] T. Koskentalo, L. Niisto, G. Blasse, J. Less-common Met. 112 (1985) 67.
[5] R. Cheng, J. Huang, Y. Xu, J. Fudan Univ. (Natur. Sci.) 28 (1989) 304.
[6] H.V. Lauer Jr., F.K. Fong, J. Chem. Phys. 65 (1976) 3108.
[7] A. Gros, F. Gaume, J.C. Gacon, J. Solid State Chem. 36 (1981) 324.
[8] P.P. Sorokin, M.J. Stevenson, J.R. Lankard, G.D. Pettit, Phys. Rev. 127 (1962) 503.
[9] A. Meijerink, J. Nuyten, G. Blasse, J. Lumin. 44 (1989) 19.
[10] G. Blasse, G.J. Dirksen, A. Meijerink, Chem. Phys. Lett. 167 (1990) 41.
[11] G.H. Dieke, in: H.M. Crosswhite, H. Crosswhite (Eds.), Spectra and Energy Levels of Rare earth Ions in Crystals, Wiley, New York, 1968.
[12] G. Blasse, Int. Rev. Phys. Chem. 11 (1992) 71.
[13] C.W. Struck, W.H. Fonger, J. Chem. Phys. 60 (1974) 1988.
[14] K. Huang, A. Rhys, Proc. Roy. Soc. (London) A 204 (1950) 406.
[15] S. Peker, Zh. Eksp. Teor. Fiz. 20 (1950) 510.
[16] W. Bron, W. Heller, Phys. Rev. 136 (1964) A1433.
[17] C.E. Weir, R.A. Schroeder, J. Res. NBS. A 68 (5) (1964) 465.
[18] F. Fong, H. Lauer, C. Chilver, M. Miller, J. Chem. Phys. 63 (1975) 366.